In Situ Observation of Monolayer Structures of Underpotentially Deposited Hg on Au(111) with the Atomic Force Microscope

Chun-hsien Chen and Andrew A. Gewirth[a]

Department of Chemistry, University of Illinois, 505 S. Mathews Avenue, Urbana, Illinois 61801

(Received 21 November 1991)

The structures of monolayers of Hg atoms underpotentially deposited on Au(111) were resolved with the atomic force microscope. In sulfate, nitrate, and perchlorate electrolytes, a hexagonal overlayer with a 0.58 ± 0.02-nm spacing was seen. In acetate, a hexagonal lattice exhibiting a 0.74 ± 0.05-nm spacing was observed positive of the underpotential-deposition potential, a rhombic lattice with a 0.43 ± 0.02-nm spacing was seen at intermediate potentials, and another hexagonal lattice with a 0.30 ± 0.03-nm spacing was found just positive of bulk deposition.

PACS numbers: 68.55.−a, 82.45.+z

Development of a detailed understanding of the structure of the electrified solid-liquid interface is a central step in understanding electrochemical reactivity. A fundamental example of this reactivity is the deposition of a monolayer of one metal onto another. This phenomenon, known as underpotential deposition (UPD) [1], occurs when metal ions are electrodeposited onto a (different) metal surface at potentials positive from the reversible (Nernst) potential. In this process, only a monolayer or submonolayer of the metal forms on the electrode surface. The structure of these monolayers has attracted considerable attention because of their importance in electrodeposition and electrocatalytic [2] processes.

In UHV environments, monolayers of foreign metal adatoms evaporated onto (111) surfaces exhibit close-packed incommensurate structures [3,4]. These close-packed structures arise from net attractive forces between the adatoms. The demonstration that UPD monolayers of Cu [5,6] and Ag [7] form open adlattice structures in the electrochemical environment has been taken to imply that the force between adatoms has become repulsive, possibly deriving from coadsorption of electrolyte with the metal. Alternatively, other effects could also serve to open the adlattice. In particular, retention of a partial charge on the adatom, complex formation with the electrolyte, or deposition of a non-fcc element onto a (111) surface of an fcc material could all lead to open lattices.

In this Letter, we report an atomic force microscope (AFM) [8] structural study of UPD of Hg onto Au(111) surfaces in four different electrolytes. The Hg UPD process is particularly important because of the technical significance of Hg amalgams and Hg surfaces in electrochemical and other processes. Underpotential deposition of Hg has been studied extensively with standard electrochemical techniques [9–15], but fundamental insight has been elusive because of the lack of microscopic surface structural information. In addition, the sensitivity of this process to different electrolytes is unknown. This latter point is important because UPD lattices of Cu [5,6] and Ag [7] on Au(111) surfaces exhibit strong electrolyte sensitivity.

AFM images were obtained with a Nanoscope II AFM [16] operating in constant force mode. The force, optimized for each image, was nominally 1×10^{-9} N. A cell made from glass held the electrolyte. Au(111) electrodes were prepared by evaporation onto cleaved mica pieces in a bell jar [17]. A Hg/Hg_2SO_4 reference electrode was affixed to the AFM glass cell with a Luggin capillary and all potentials are referred to this electrode. A gold wire, cleaned by polarization in another cell and flame annealed prior to every experiment, was used as the counter electrode.

Electrolytes were prepared by dissolving HgO into the appropriate acid followed by dilution to yield solutions which were 1 mM in Hg and 0.1 M in the acid. Water was from a Millipore-*Q* purification system. The acetic acid electrolyte had 0.1-M sodium acetate added to increase its conductivity. Solutions were deoxygenated with Ar prior to use.

A cyclic voltammogram (CV) obtained in a solution containing 1-mM HgO in 0.1-M H_2SO_4 is shown in Fig. 1(a). Identical voltammetry was obtained in nitrate and

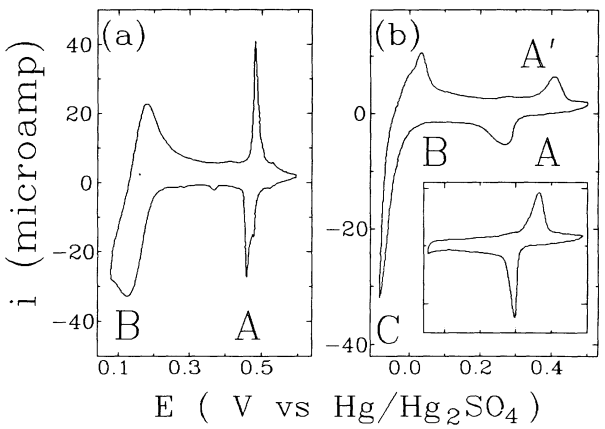

FIG. 1. Cyclic voltammograms obtained with a sweep rate of 20 $mV s^{-1}$ for Hg UPD onto Au(111) in (a) 0.1-M H_2SO_4 containing 1-mM Hg and (b) 0.1-M CH_3COOH, 0.1-M CH_3COONa, and 1-mM Hg. Inset to (b): Voltammetry for the most anodic UPD peak at a sweep rate of 2 $mV s^{-1}$.

perchlorate electrolytes. The first UPD peak (A) occurs at +460 mV and the maximum current of the second UPD peak (B) was at ~+130 mV. This voltammetry is quite similar to that reported previously [11], with the exception that only two UPD peaks are seen when the negative potential excursion is limited to +60 mV. More negative of this potential, an alloy is formed with the Au surface, leading to roughening and substantial morphological changes when it is stripped [18]. The published voltametric behavior could also be recovered when the Au(111) surface was roughened by electrochemical oxidation [19] prior to the UPD cycle, indicating that the additional peaks seen previously are due to surface modification.

Voltammetry for Hg UPD in acetate electrolyte is shown in Fig. 1(b). There are three major differences in the voltammetic behavior in this electrolyte relative to the others studied here. First, at a scan rate of 20 mV s^{-1}, the first UPD peak (A) in acetate is substantially broader than the corresponding peak in the other electrolytes (60 vs 20 mV). Second, the difference in potential between this peak and the corresponding stripping peak is about 140 mV, while the corresponding difference in the other electrolytes was no more than 25 mV with the same sweep rate. Slowing the sweep rate [Fig. 1(b), inset] causes the stripping and deposition peaks to move closer together, indicating the presence of a substantial kinetic effect for monolayer formation. The final difference between voltammetry in acetate and the other electrolytes was the behavior of peak B near the bulk deposition potential where this peak was not as distinct from the bulk in acetate as it was in the other three electrolytes.

Atom-resolved images in sulfate, nitrate, or perchlorate electrolyte were seen only just prior to and just after bulk deposition. However, prior to the addition of Hg, we always observed the characteristic Au(111) corrugation [20] which disappeared as soon as even small amounts of the metal were introduced. This behavior stands in contrast to that observed in Ag [7] or Cu [6] on Au(111) UPD systems where Au(111) corrugation was observed at potentials positive of the UPD potential even with the UPD adatom in solution. The absence of corrugation in the presence of Hg at positive potentials is possibly due to formation of a fluxional Hg complex on the Au surface, which interferes with the imaging mechanism.

At +47 mV, positive of the reversible potential, a hexagonal structure exhibiting a 0.58 ± 0.02-nm spacing was observed [Fig. 2(a)]. The large spacing suggests the presence of very strong repulsive forces between adatoms on the surface. Essentially the same images, in the same potential region, were observed in nitrate and perchlorate electrolytes.

More negative of this potential, at −45 mV, we saw [Fig. 2(b)] a different image. Here, we observed a hexagonal structure with an atom-atom spacing of 0.29 ± 0.03 nm. This distance is consistent with both the Au(111) (0.288 nm) and frozen Hg (0.301 nm) lattice

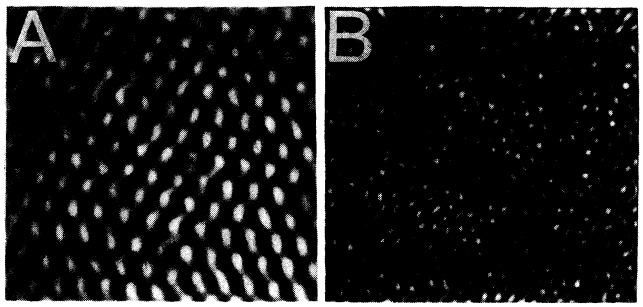

FIG. 2. 7×7-nm AFM images of Hg UPD onto Au(111) in sulfate obtained (a) at +47 mV vs $Hg/HgSO_4$ exhibiting an atom-atom spacing of 0.58 ± 0.02 nm and (b) at −45 mV vs $Hg/HgSO_4$ where a 0.29 ± 0.03-nm atom-atom spacing is obtained.

spacings. However, solid Hg exhibits a rhombohedral lattice, and thus the hexagonal surface structure is not expected. Hg and Au are known to alloy in this potential region [11], and the structure we observe may be that of the alloy, which reflects the dominant Au contribution. We note that AFM images obtained in this potential region were not as clear as those of bare Au(111) [20], Ag(111) [7], and Cu(111) [6] surfaces obtained in other experiments.

Completely different lattices were observed in acetate, which is consistent with the substantial voltammetric differences observed in this electrolyte.

Positive of the first UPD peak we saw [Fig. 3(a)] a hexagonal structure exhibiting an extremely large 0.74 ± 0.05-nm spacing which is about 2.5 times the Au(111) atom-atom spacing. This lattice clearly is not the 0.29-nm hexagonal Au(111) lattice expected in this potential region, and its existence positive of the first UPD peak suggests that a complex is formed between Hg(II) and the acetate electrolyte. If Hg was not present in the solution, then only the Au(111) lattice was seen. The 0.74-nm lattice persisted in solution with positive potential sweeping until the onset of oxide formation. Formation of a less stable complex may be responsible for the lack of resolution observed in the other three electrolytes in this potential region.

Figure 3(b) shows the lattice observed at potentials between the first and second UPD peaks (between peaks A and B). This structure is clearly rhombic, with a 0.43 ± 0.02-nm atom-atom spacing and 81° ± 3° and 99° ± 3° angles. We could clearly see the change from the large, open lattice positive of the first UPD peak to this more close-packed lattice with potential sweeping.

Finally, if the potential was ramped to even more negative values, just prior to bulk deposition, negative of peak B in Fig. 1, the surface structure changed again and a hexagonal lattice appeared [Fig. 3(c)]. The atom-atom spacing here is 0.31 ± 0.02 nm which is consistent with either the frozen Hg or the Au(111) lattices.

Further insight into the structures observed in the

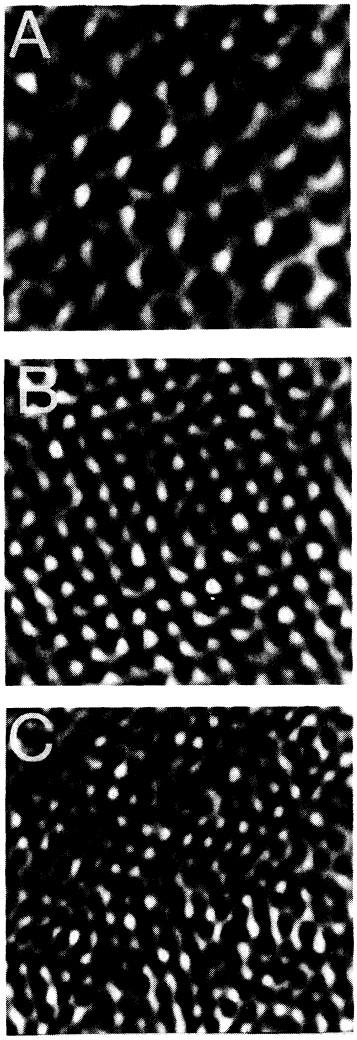

FIG. 3. 5×5-nm AFM images of Hg UPD onto Au(111) in acetate obtained (a) prior to UPD at +356 mV showing a spacing of 0.74 ± 0.05 nm, (b) at +143 mV exhibiting a rhombic lattice with a 0.43 ± 0.02-nm spacing, and (c) at −48 mV displaying a 0.31 ± 0.02-nm hexagonal lattice.

Hg/Au(111)/acetate UPD system is obtained from a potential jump experiment. Here, the potential was stepped from −47 mV, just positive of bulk deposition, to +345 mV, positive of the first UPD peak. Starting from the close-packed structure [Fig. 3(c)], the image became cloudy and then briefly settled into a close-packed hexagonal structure with a 0.29-nm atom-atom spacing. After approximately 15 s, this image was again obscured and the 0.74-nm hexagonal structure, seen at the start of the experiment, appeared. The temporal behavior of the AFM images is consistent with the voltametric response, shown in the inset in Fig. 1(b), which also suggested kinetically hindered formation of the adlattice observed with the AFM.

This work shows that a number of different factors are responsible for the monolayer structures observed during UPD.

The Hg UPD adlattice on Au(111) exhibits relatively little electrolyte sensitivity. The one structure observed in sulfate, perchlorate, or nitrate electrolytes exhibits a hexagonal structure and an extremely large atom-atom spacing of 0.58 nm. This spacing is substantially larger than the frozen Hg lattice spacing of 0.31 nm [21] and is also much larger than what is thought to be the average Hg-Hg spacing (0.325 nm) in the liquid metal [22]. The hexagonal structure is also surprising, as Hg forms a rhombohedral lattice in its crystalline state. Monolayer deposits of Bi, another rhombohedral material, form a rhombic structure on Ag(111) surfaces [23].

Insight into the Hg UPD system in sulfate, nitrate, and perchlotate electrolytes is reasonably obtained by reference to previous electrochemical studies. There is general agreement that only 1.6 [10] to 1.8 [12] electrons are consumed during monolayer formation from Hg(II) solutions. This means that a substantial positive charge is left on the Hg adatom which could provide the repulsive force necessary to open the structure. A hexagonal lattice is the two-dimensional structure expected from point charge repulsion between adatoms, which may explain why a hexagonal rather than a rhombic structure is observed. This model also accounts for the reduced sensitivity of the UPD adlattice to the electrolyte, as the adatoms are already quite well separated and any additional forces arising from the anions would be minimal relative to Coulombic forces from the adatoms themselves.

In acetate electrolyte, a novel structural change going from hexagonal to rhombic to hexagonal is observed. This change may reflect the affinity of Hg for the acetate ligand [24] and imply that the structures observed on the Au(111) surface are really indicative of complex formation. The observed structures may be a manifestation of anion-induced cation adsorption which has been studied in detail on Hg electrode surfaces [25]. We then associate the structure observed positive of the first UPD peak with Hg(II) acetate, the rhombic intermediate structure with Hg(I) acetate, and the final structure with a close-packed monolayer occurring after stripping the final acetate ligand. We note that a decrease in Hg-Hg distance and a consequent increase in packing density on the electrode surface is expected on going from Hg(II) diacetate to Hg(I) monoacetate, but there is at this time no crystal structure of the mecurous form available.

In summary, we have observed UPD monolayers formed by Hg in four different electrolytes. In three of these, an open hexagonal structure is observed which is reasonably associated with the substantial partial charge remaining on the Hg adatom. In acetate electrolyte, complexation effects between the adatom and the anion appear to dominate, and this system thus represents a novel type of UPD.

C.-h.C. acknowledges a University of Illinois Fellowship in Chemistry. A.A.G. acknowledges a Presidential

Young Investigator Award with matching funds provided by Digital Instruments, Inc. This work was funded by the Department of Energy, Grant No. DEFG02 91 ER45439, through the Materials Research Laboratory at the University of Illinois.

[a]Author to whom correspondence should be addressed.

[1] D. M. Kolb, in *Advances in Electrochemistry and Electrochemical Engineering*, edited by H. Gerischer and C. W. Tobias (Wiley-Interscience, New York, 1978), Vol. 11, p. 125.

[2] R. Adzic, in *Advances in Electrochemistry and Electrochemical Engineering*, edited by H. Gerischer and C. W. Tobias (Wiley-Interscience, New York, 1984), Vol. 13, p. 159.

[3] D. D. Chambliss and R. J. Wilson, J. Vac. Sci. Technol. B **9**, 928 (1991).

[4] M. M. Dovek, C. A. Lang, J. Nogami, and C. F. Quate, Phys. Rev. B **40**, 11973 (1989).

[5] O. M. Magnussen *et al.*, Phys. Rev. Lett. **64**, 2929 (1990).

[6] S. Manne *et al.*, Science **251**, 183 (1991).

[7] C.-H. Chen, S. M. Vesecky, and A. A. Gewirth, J. Am. Chem. Soc. **114**, 451 (1992).

[8] G. Binnig, C. F. Quate, and C. Gerber, Phys. Rev. Lett. **56**, 930 (1986).

[9] R. W. Andrews, J. H. Larochelle, and D. C. Johnson, Anal. Chem. **48**, 212 (1976).

[10] T. R. Lindstrom and D. C. Johnson, Anal. Chem. **53**, 1855 (1981).

[11] L. A. Schadewald *et al.*, J. Electrochem. Soc. **131**, 1583 (1984).

[12] W. G. Sherwood and S. Bruckenstein, J. Electrochem. Soc. **125**, 1098 (1978).

[13] W. G. Sherwood, D. F. Untereker, and S. Bruckenstein, J. Electrochem. Soc. **125**, 384 (1978).

[14] M. Shay and S. Bruckenstein, Langmuir **5**, 280 (1989).

[15] G. Salie, J. Electroanal. Chem. **259**, 315 (1989).

[16] Digital Instruments 6780 Cortona Drive, Santa Barbara, CA 93117.

[17] Evaporation parameters, pressure $< 2\times10^{-6}$ torr, mica temperature 300 °C, evaporation rate 0.1 nm/s.

[18] I. C. Oppenheim *et al.*, Science **254**, 687 (1991).

[19] D. J. Trevor, C. E. D. Chidsey, and D. N. Loiancono, Phys. Rev. Lett. **62**, 929 (1989).

[20] S. Manne, H.-J. Butt, S. A. C. Gould, and P. K. Hansma, Appl. Phys. Lett. **56**, 1758 (1990).

[21] C. S. Barrett, Acta Crystallogr. **10**, 58 (1957).

[22] J. S. Lukesh, W. H. Howland, L. F. Epstein, and M. D. Powers, J. Chem. Phys. **23**, 1923 (1955).

[23] M. F. Toney *et al.*, Langmuir **7**, 796 (1991).

[24] R. Allmann, Z. Kristallogr. **138**, 366 (1973).

[25] M. Aihara and F. C. Anson, J. Electroanal. Chem. **99**, 55 (1979), and references therein.

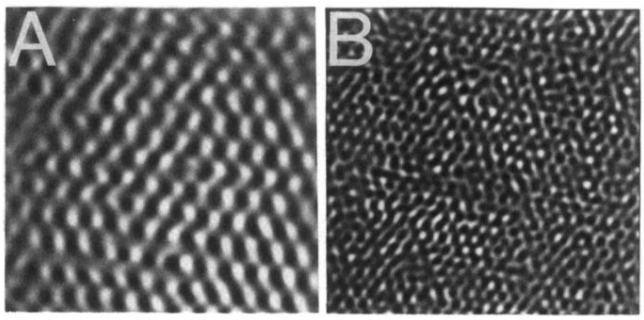

FIG. 2. 7×7-nm AFM images of Hg UPD onto Au(111) in sulfate obtained (a) at +47 mV vs $Hg/HgSO_4$ exhibiting an atom-atom spacing of 0.58 ± 0.02 nm and (b) at −45 mV vs $Hg/HgSO_4$ where a 0.29 ± 0.03-nm atom-atom spacing is obtained.

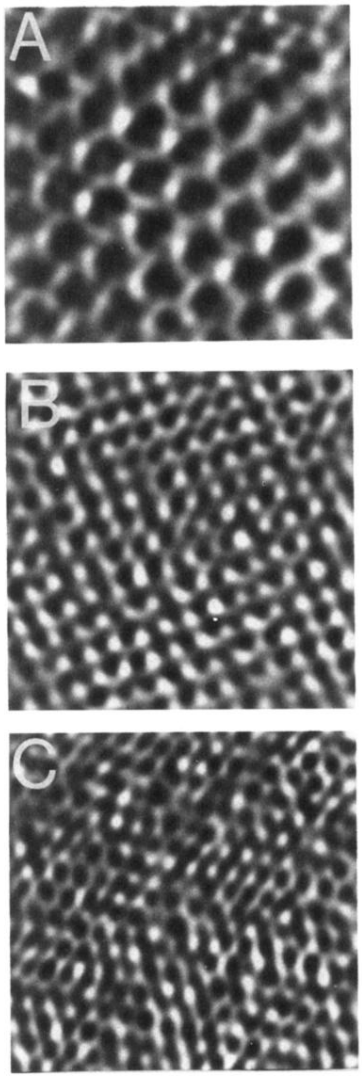

FIG. 3. 5×5-nm AFM images of Hg UPD onto Au(111) in acetate obtained (a) prior to UPD at +356 mV showing a spacing of 0.74 ± 0.05 nm, (b) at +143 mV exhibiting a rhombic lattice with a 0.43 ± 0.02-nm spacing, and (c) at −48 mV displaying a 0.31 ± 0.02-nm hexagonal lattice.